# The effect of adjacent clay layers and seams on the ultimate base resistance of piles in sand

Xiangtao Xu and Barry Lehane
School of Civil and Resource Engineering, the University of Western Australia

Keywords: soil layering, pile, end bearing resistance, two-layer, three-layer

**ABSTRACT**

This paper presents the results of numerical analyses that investigated the reduction in pile/cone installation end-bearing resistance in a sand layer due to the presence of adjacent weaker clay layers. It is assumed that the ultimate end-bearing resistance of a penetrometer (cone or pile) can be related to the expansion of a spherical cavity. A number of two and three layered soil systems were examined using the Plaxis finite element code. It is shown that the reduction in pile/cone installation end-bearing resistance in strong soil depends on the relative distance from the layer interface, the thickness of the weak soil layer and the stiffness and strength difference between the strong and weak soil. Correction factors that cater for the influence of the weaker soil are recommended.

## 1 INTRODUCTION

In the 40th Terzaghi lecture, Poulos [2005] concluded that the natural imperfections, such as the existence of weak compressible soil layers in the vicinity of a pile tip, can create significant problems for a piled foundation and lead to a reduction in both capacity and stiffness of a single pile and pile group. However, despite its importance for pile design, the effects of soil layering on a pile/cone end-bearing resistance are not adequately addressed in literature.

Previous research includes small-scale laboratory tests and numerical analysis [Ahmadi & Robertson 2005, Meyerhof 1983]. In particular, the simplified linear elastic approach [Vreugdenhil et al. 1994, Yue & Yin 1999] is shown by other researchers [Berrill et al. 2004, Joer et al. 1996] to capture the general feature of the layering effects on the pile/cone steady state tip resistance (q). This method is also recommended in Lunne et al. [1997] as a means of assessing the effects of soil layering. Such recognition should, however, be treated with caution. For example, the method predicts that a standard cone (diameter D=0.036m) in dense sand (with CPT $q_c$ ~10 MPa) continues to sense the presence of an overlying soft clay layer (with CPT $q_c$ ~0.1MPa), even after penetrating a depth of 16m into the dense sand; the significant extent of this predicted zone of influence is not realistic. The inadequacy of the simplified linear elastic approach was also demonstrated by Ahmadi & Robertson [2005] and Youd et al. [2001].

In this paper, the pile/cone penetration is simulated by assuming the spherical cavity expansion analogue which relates the pile/cone steady state penetration resistance (q) to the cavity limiting pressure ($p_{limit}$). The Plaxis finite element computer code [Brinkgreve et al. 2004] was used to model the process of a cavity expansion in layered soil profiles. The hardening soil (HS) model [Schanz et al. 1999] was employed to simulate both dense sand and soft clay. The paper extends the numerical and experimental research presented by Xu & Lehane [2007] for a two layer system.

## 2 NUMERICAL MODEL IN PLAXIS

### 2.1 Soil profiles and parameters

It is clearly desirable that end bearing piles extend a sufficient distance away from any overlying weak layers to avoid potential reductions in pile base stiffness and capacity. However, this may not always be possible for a number of practical reasons, including those imposed by the selected pile driving equipment. Figure 1 shows a sketch of a number of possible pile embedment situations. The steady state penetration resistance in a given strong soil layer ($q_S$) is expected to reduce due to the presence of weaker soil layers close to pile tip level. In other words, the resistance in layered soil profiles (e.g. $q_{WS}$, $q_{WSW}$, $q_{SWS}$ as defined in Figure 1) are lower than $q_S$ at the same penetration depth. In a two-layer soil (Figure 1b), the reduction in resistance (i.e. $q_{WS}/q_S$) depends on the distance from pile tip level to the layer interface (H), and also the relative stiffness and strength difference between the weak and strong soil; in a three-layer soil profile, an additional parameter, $T_S$ (the thickness of the strong soil layer, Figure 1c) or $T_W$ (the thickness of the weak soil layer, Figure 1d), are also likely to play an important role in determining the available resistance.

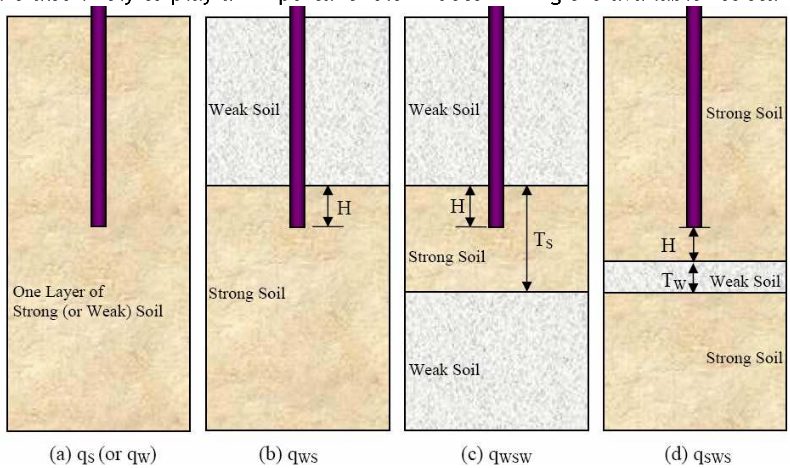


Figure 1: Soil profiles (a) strong (or weak) soil only, $q_S$ (or $q_W$), (b) weak over strong, $q_{WS}$, (c) weak over strong over weak, $q_{WSW}$, (c) strong over weak over strong, $q_{SWS}$

In this study, the strong and weak soils are represented by dense (free-draining) sand and (undrained) clay with soil parameters specified for the hardening soil (HS) model. The HS model is described in detail by Schanz et al. [1999] and incorporates features such as (i) stress and strain level dependency of stiffness, (ii) shear and volumetric hardening, and (iii) a limitation on dilation when the maximum void ratio is reached. Table 1 summarises the soil parameters employed for the sand and the clay. The reader is referred to Schanz et al. [1999] or the Plaxis reference manual [Brinkgreve et al. 2004] for a full description of these parameters.

Table 1: The soil parameters of HS model

| Soil parameters | Dense sand | Clay |
|---|---|---|
| $E_{50}^{ref}$, (MPa) | 100 | 5 |
| $E_{ur}^{ref}/E_{50}^{ref}$ | 3 | 3 |
| $E_{oed}^{ref}/E_{50}^{ref}$ | 1 | 1 |
| Poisson's ratio, $\nu$ | 0.2 | 0.2 |
| Earth pressure at rest, $K_0$ | 1 | 1 |
| Saturated unit weight, $\gamma_{sat}$, (kN/m$^3$) | 20 | 20 |
| Cohesion, c, (kPa) | 0.2 | 0.2 |
| Friction angle, $\phi$ (°) | 42 | 20 |
| Dilation angle, $\psi$ (°) | 12 | 0 |
| Stress dependency exponent, m | 0.5 | 1.0 |
| Initial void ratio, $e_{initial}$ | 0.5 | - |
| Maximum/minimum void ratio, $e_{max}$ & $e_{min}$ | 0.78 & 0.49 | - |
| Relative density, $D_r$ | 97% | - |
| Drainage | Drained | Undrained |

## 2.2 Numerical mesh and analysis procedures

All calculations were performed using an axisymmetric mesh with a height of 24m and height of 12m and comprising triangular elements each with 15 nodes and 12 Gauss points. A typical mesh in a two-layer soil profile is shown in Figure 2. The spherical cavity, which was represented by a linear elastic soil cluster with an initial radius of 0.1m (referred as $a_0$), was fixed at a depth of 12m ($\sigma'_{v0}$=120kPa with water at ground surface). Expansion of the cavity was achieved by applying positive volumetric strain to the spherical soil cluster. The expanding pressure relationship with radial displacement was obtained by selecting appropriate nodes and gauss points for output by the program. In this study, the layer interfaces were altered with reference to the location of the centre of the cavity at a depth of 12m to simulate the penetration of a pile/cone, as were changes in layer thickness (i.e. $T_S$ & $T_W$).

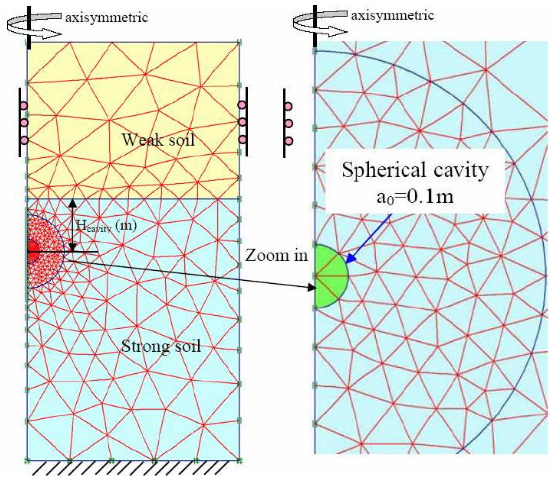


Figure 2: Typical mesh for a spherical cavity expansion in a two-layer soil profile in PLAXIS

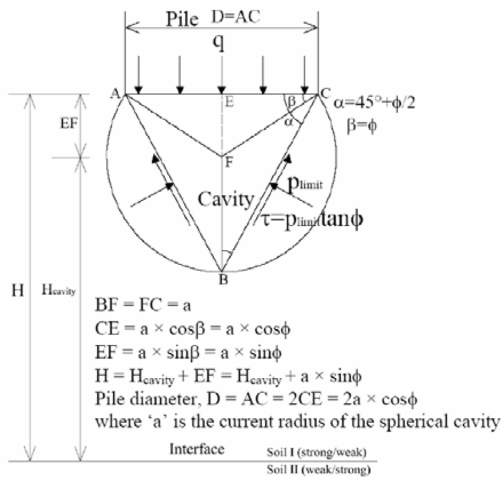


Figure 3: Schematic diagram of relationship between geometry of the cavity and the pile [Xu & Lehane 2007]

Figure 3 shows the relationship between a pile of diameter 'D' and a cavity of current radius 'a' [Xu & Lehane 2007]. Firstly, based on the vertical force equilibrium on the soil wedge beneath the pile tip, the steady state penetration resistance q can be related to cavity limit pressure $p_{limit}$ as follows:

$$q = p_{limit}\,(1 + \tan\alpha \times \tan\phi') \qquad (1)$$

where $\phi'$ is the internal angle of friction and $\alpha$ equals to 60° for a standard cone penetrometer, but can be taken as $(45+\phi/2)$ for a pile [Randolph et al. 1994].

The distance from the pile tip to the layer interface (H) can be expressed as a function of the distance from the centre of the cavity to the layer interface ($H_{cavity}$), current cavity radius (a), and soil friction angle ($\phi$). The normalised distance to the layer interface (H/D) can therefore be evaluated as:

$$H/D = H_{cavity} / (2a \times \cos\phi) + 0.5 \times \tan\phi \qquad (2)$$

where $H_{cavity}$ is positive in strong soil and negative in weak soil.

The analysis procedure to model a spherical cavity expansion in PLAXIS is briefly discussed here. Full details are given by Xu & Lehane [2007]. It can be divided into five sequential steps: (i) "input", including mesh set-up and initial stress generation (ii) "calculate", including defining calculation phases and selecting nodes and stress points for output, (iii) "output", including extracting data using the PLAXIS curve program, post-processing data to generate pressure expansion curves and evaluation of the limit pressure $p_{limit}$ and corresponding radial displacement 'u' (-and therefore current radius 'a', $a=a_0+u$) (iv) calculation of steady state resistance q (e.g. $q_S$, $q_W$, $q_{WS}$, $q_{WSW}$, $q_{SWS}$) from $p_{limit}$ (Equation 1), and (v) evaluate the reduction in resistance as a function of H/D (Equation 2) in a two-layer soil (e.g. $q_{WS}/q_S$ vs. H/D) or a function of H and $T_S$ (or $T_W$) in a three-layer soil.

## 3 RESULTS IN LAYERED SOIL

### 3.1 Clay over dense sand

The resistance in the two-layer soil ($q_{WS}$) as shown in Figure 1b can be compared with that in a one layer strong soil ($q_S$) using the procedures outlined. The reduction in resistance ($q_{WS}/q_S$) in dense sand due to the presence of overlying clay layer was evaluated as a function of normalised distance from the layer interface (H/D) and these predictions are summarised in Figure 4. It is shown that the steady state resistance ratio between the clay and the dense sand ($q_W/q_S$) is around 0.02. There is only a slight increase in resistance before the pile penetrates the underlying dense sand and the zone of influence over which resistances exceed the steady state values in the clay is only ~1D. This finding is consistent with other research findings [Meyerhof 1983, Ahmadi & Robertson 2005] indicating that the zone of influence in weak soil ($Z_W$) is generally less than 2 times pile diameters. However, as seen on Figure 4, a much greater distance into the underlain dense sand is required before the pile stops sensing the overlying soft clay. The $q_{WS}/q_S$ ratio only reaches unity at a penetration depth of 14D into the dense sand layer i.e. the zone of influence in the dense sand ($Z_S$) is ~14D, which is much greater than that in the clay (i.e. <2D). This relatively large zone of influence is consistent with experimental data obtained in centrifuge tests reported by Xu & Lehane [2007], who also show that the value of $Z_s$ decreases as $q_{ws}/q_s$ increases.

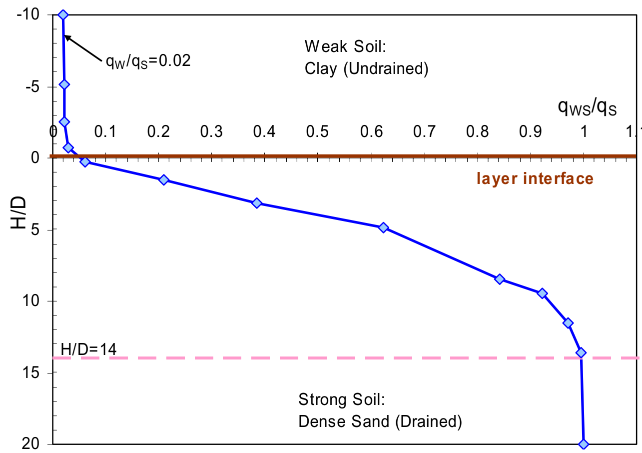


Figure 4: Schematic diagram of relationship between geometry of the cavity and the pile

### 3.2 Dense sand layer within overlying and underlying clay

As shown in Figure 1c, the three-layer system comprises a middle dense sand layer underlain and overlain by soft clay. Compared to the two-layer soil profile in Figure 1b, there is an additional underlying weak layer. Therefore, the resistance in the dense sand will reduce further due to the introduction of this clay layer. As the thickness of the dense sand layer increases, the resistance reduction factors ($q_{SWS}/q_S$) in the strong soil will be the same as those in a two-layer soil profile ($q_{WS}/q_S$). To investigate the additional reduction in resistance compared to a two-layer soil (i.e. $q_{SWS}/q_{WS}$), one series of analyses were performed in which both H and $T_S$ were varied.

The results are summarised in Figure 5, in which the further reduction in resistance, $q_{WSW}/q_{WS}$, in the dense sand, is plotted against the normalised thickness of the dense sand, ($T_S$-2H)/D at varying H/D values. For this case, the reduction in resistance $q_{WSW}/q_S$ is determined as:

$$q_{WSW} / q_S = (q_{WS} / q_S) \times (q_{WSW} / q_{WS}) \tag{3}$$

Ratios of $q_{WSW}/q_{WS}$ at certain H/D values increase rapidly with ($T_S$-2H)/D and exceed 0.95 at ($T_S$-2H)/D values in excess of about 3. The lowest resistance reduction factor ($q_{WSW}/q_{WS}$=0.85) occurs when the pile tip is embedded near the middle of a relatively thin strong soil layer. In summary, to evaluate $q_{WSW}/q_S$ there are two steps to follow: (i) choose the distance closest to the interfaces as H, based on which, the resistance reduction factor ($q_{WS}/q_S$) in a two-layer soil profile can be first evaluated (e.g. Figure 4); and (ii) evaluate the additional resistance reduction factor ($q_{WSW}/q_{WS}$) due to another weak layer (e.g. Figure 5). The final resistance reduction factor ($q_{WSW}/q_S$) is therefore given as in Equation 3. It is noted that in a three-layer soil profile, the most critical evaluation of the resistance reduction depends on the $q_{WS}/q_S$ ratio in a two-layer soil profile, which could range from as low as 0.01 to 1.0, while the further resistance reduction factors of $q_{WSW}/q_{WS}$ are in general greater than 0.85 for a ratio of $q_{WS}/q_S$ as low as 0.02.

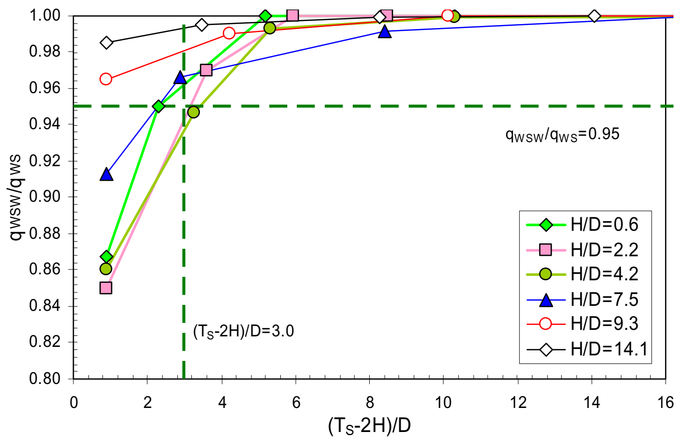


Figure 5: Further reduction in resistance compared to weak over strong

### 3.3 Clay seam within sand deposit

The existence of a clay seam below the pile tip can significantly reduce pile base capacity (and stiffness). As shown in Figure 1d, the three-layer soil system consists of a clay layer embedded in the middle of two dense sand layers. The thickness of the weak layer ($T_W$) is as critical as the distance to the interface (H) in controlling the magnitude of the ultimate pile base resistance. The resistance ($q_{SWS}$) at a certain distance will increase to the unaffected resistance ($q_S$) in strong soil as the thickness of the weak layer reduces to zero. To quantify this effect, one series of PLAXIS analyses was performed by varying both H and $T_W$.

The results obtained from these analyses are summarised in Figure 6. The calculated resistance $q_{SWS}$ in this three-layer soil profile can be compared with the unaffected resistance in a single layer of dense sand ($q_S$). It is clear that resistance reduction factors $q_{SWS}/q_S$ depend on the thickness of the weak layer ($T_W$) and also on the normalised distance from the pile tip to the interface (H/D). In general, for a thickness $T_W$ > 3D, the $q_{SWS}/q_S$ ratios are approaching the $q_{WS}/q_S$ values (in a two-layer soil profile). This implies that the reduction in resistance ($q_{SWS}/q_S$) in such a three-layer soil can be conservatively assumed equal to that ($q_{WS}/q_S$) in a two-layer soil provided the thickness of the weak soil ($T_W$) is greater than 3D.

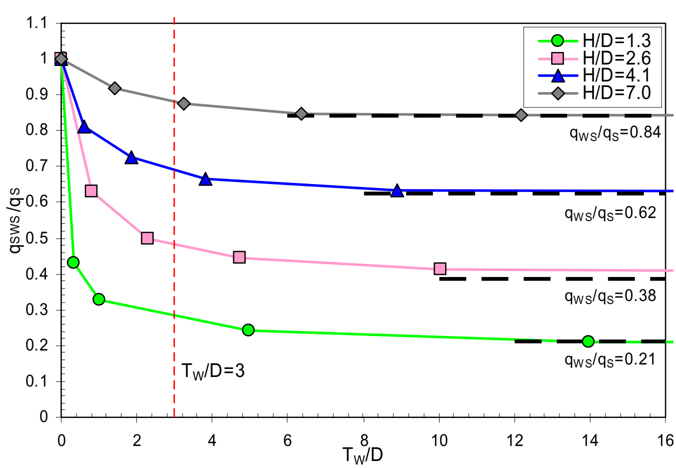


Figure 6: Reduction in resistance due to the underlain clay seam

## 4 CONCLUSIONS

The FE analyses presented in this paper, which employed a realistic constitutive model for the soil, quantify the relative reduction in penetration resistance that a pile/penetrometer in dense sand experiences due to the presence of neighbouring weak clay layers. For the case of clay over dense sand, the zone of influence in the dense sand extends up to 14 times pile diameters. Once the pile enters the clay, the resistance is largely independent of the soil properties of the dense sand. For a pile end bearing in a dense sand layer that is underlain and overlain by soft clay layers, it was found that further reduction in resistance compared to the clay over sand case is relatively small. For the case of a clay seam in the vicinity of the pile base in sand, the reduction in resistance is shown to be comparable to that experienced in a two-layer soil comprising sand over clay with thickness of the clay greater than 3D.

## REFERENCES


Ahmadi, M. M. and Robertson, P. K. (2005). *Thin-layer effects on the CPT $q_c$ measurement*. Can. Geotech. J. 42(5), 1302-1317

Berrill, J. b., Canou, J., Le Kouby, A., and Foray, P. (2004). *The effect of layering on cone resistance: calibration chamber tests*. In Proceedings of 9th Australia New Zealand Conference on Geomechanics, Auckland, 648-653

Brinkgreve, R.B.J., Broere,W. and Waterman D. (ed.) (2004). Plaxis 2D-Version8. Plaxis B.V., Balkema, Rotterdam

Joer, H. A., Randolph, M. F., and Liew, Y. H. (1996). *Interpretation of cone resistance in layered soils*. In Proceedings of 7th Australia New Zealand Conference on Geomechanics, Adelaide, 92-97

Lunne, T., Robertson, P. K., and Powell, J. J. M. (1997). *Cone penetration testing in geotechnical practice*. Blackie Academic & Professional, London

Meyerhof, G. G. (1983). *Scale effects of ultimate pile capacity*. J. Geotech. Engng. ASCE, 109(6), 797-806

Poulos, H.G. (2005). *Pile behaviour - Consequences of geological and construction imperfections*. Journal of Geotechnical and Geoenvironmental Engineering. 13(5), 538-563

Randolph, M. F., Dolwin, J., and Beck, R. *Design of driven piles in sand*. Geotechnique Vol. 44, No. 3, (1994) 427-448

Schanz, T., Vermeer, P. A., and Bonnier, P. G. (1999). *The hardening soil model: formulation and verification*. In Beyond 2000 in Computational Geotechnics - 10 Years of Plaxis, Rotterdam, 1-16

Vreugdenhil, R., Davis, R., and Berrill, J. (1994). *Interpretation of cone penetration results in multilayered soils*. Int. J. Numer. Anal. Methods in Geomech. 18(9), 585-599

Xu, X. and Lehane, B.M. (2007). *Pile and penetrometer end bearing resistance in two-layered soil profiles*. Submitted to Geotechnique in Dec. 2006

Xu, X. (2007). *Investigation of the end bearing performance of displacement piles in sand*. PhD thesis, the University of Western Australia

Youd, T. L., Idriss I. M., Andrus, Ronald D., Arango, Ignacio, Castro, Gonzalo, Christian, John T., et al. (2001). *Liquefaction resistance of soils: summary report from the 1996 NCEER and 1998 NCEER/NSF workshops on evaluation of liquefaction resistance of soils*. J. Geotech. Geoenviron. Engng. 127(10), 817-833

Yue, Z.Q. and Yin, J.H. (1999). *Layered elastic model for analysis of cone penetration testing*. Int. J. Numer. Anal. Methods in Geomech. 23, 829-843